Comparison between dominant NBI and dominant IC heated ELMy H-mode discharges in JET

R. Sartori [1], T.W. Versloot [2], P.C. de Vries [2], F. Rimini [3], G. Saibene [1], V. Parail [4], M. Beurskens [4], A. Boboc [4], R. Budny [5], K. Crombe [6], E. de la Luna [7], F. Durodie [8], T. Eich [9], C. Giroud [4], V. Kiptily [4], T. Johnson [10], P. Mantica [11], M-L. Mayoral [4], D.C. McDonald [4], I. Monakhov [4], M.F.F Nave [12], I. Voitsekovitch[4], K-D. Zastrow [4] and JET EFDA Contributors*

e-mail address of lead author: Roberta.Sartori@f4e.europa.eu

JET-EFDA, Culham Science centre, OX14 3DB, Abingdon, UK
[1] Fusion For Energy Joint Undertaking, Josep Pla 2, 08019, Barcelona, Spain
[2] FOM Institute Rijnhuizen, Association EURATOM-FOM, Nieuwegein, The Netherlands
[3] JET-EFDA Close Support Unit, Culham Science centre, OX14 3DB, Abingdon, UK
[4] Euratom/CCFE Association, Culham Science Centre, Abingdon, OX14 3DB
[5] Princeton Plasma Physics Laboratory, Princeton, New Jersey 08543, USA
[6] Department of Applied Physics, Ghent University, Belgium
[7] Asociacion Euratom-CIEMAT para Fusion, CIEMAT, E28040 Madrid, Spain
[8] ERM-KMS, Euratom-Belgian State, TEC partners, Brussels, Belgium
[9] Max-Planck-Institut für Plasmaphysik, Boltzmannstrasse 2, 85748 Garching, Germany
[10] Uppsala University, Association EURATOM-VR, Sweden
[11] Istituto di Fisica del Plasma 'P.Caldirola', Associazione Euratom-ENEA-CNR, Milano, Italy
[12] Associacao EURATOM/IST, Centro de Fusao Nuclear, 1049-001 Lisbon, Portugal
* See Appendix of Romanelli et al., Fusion Energy 2010 (Proc. 23rd Int. Conf. Daejeon) IAEA (2010)

Abstract: The experiment described in this paper is aimed at characterizing of ELMy H-mode for plasmas with varying momentum input, rotation, power deposition profiles and ion to electron heating ratio obtained by varying the proportion between IC and NB heating. The motivation for the experiment was to verify that the basic confinement and transport properties of the baseline ITER H-mode are robust to these changes, and similar to those derived from the large database of NB heated H-modes. No significant difference in the density and temperature profiles or in the global confinement were found. Although ion temperature profiles were seen to be globally stiff, some variation of stiffness was obtained in the experiment by varying the deposition profiles, but not one that could significantly affect the profiles in terms of global confinement. This analysis shows the thermal plasma energy confinement enhancement factor to be independent of the heating mix, for the range of conditions explored. Moreover, the response of the global confinement to changes in density and power were also independent of heating mix, and were reflecting the changes in the pedestal, which is consistent with the profiles being globally stiff. Consistently, the pedestal characteristics (pressure and width) and their dependences were the same with NB or with predominant IC heating.

1. Introduction

Extrapolations from present day machines to the ITER Q=10 inductive standard scenario are predominantly based on ELMy H-modes heated by positive neutral beam (NB) injection, yielding a power deposition that is off-axis and mainly directed towards the ions. In ITER auxiliary heating is mainly on-axis and predominantly directed towards electrons while the standard Deuterium-Tritium scenario will be dominated by on-axis α-particle heating. The comparison of H-modes with predominant positive NB or predominant Ion Cyclotron (IC) heating can help therefore to confirm the prediction for ITER with different sources of additional heating, and in particular with respect to providing toroidal momentum input or fuelling. Input power and rotation are decoupled in H-modes with predominant IC. Previous studies at JET suggested that confinement times depended on rotation, although the difficulty was to properly decouple power and torque [1]. In JET H-modes at medium/high plasma current and density, the NB heating is deposited off axis, while IC can provide central electron heating, similar to ITER.

Previous experiments [2, 3, 4, 5] comparing predominantly IC and NB heated H-modes consistently reported no difference in energy confinement enhancement factor, H_{98}, or even an increase (<10%) in H_{98} with IC. The latter was attributed to more peaked electron temperature profiles due to more central power deposition with IC. Similarly, the H_{98}-factor did not vary significantly with T_i/T_e and the density profile shape in Hybrid scenarios with strong central IC in ASDEX Upgrade [6]. The JET results on in sawtooth-free H-mode phases, showed a tendency of electron temperature profiles to achieve invariance once the

critical inverse gradient length threshold was exceeded, when performing an electron heat flux scan by using on- and off-axis dominant IC [5]. A detailed transport analysis in [7] showed a significant effect of rotation on the stiffness of the ion temperature profiles in the inner half of the plasma. As part of the analysis, NB and IC heated H-modes were also compared, concluding that the modest variation in T_i profiles was due to the small variation of the normalised core heat flux with NB compared to IC, deriving from the less localised power deposition of NB at constant total power.

In these previous studies, the analysis of the pedestal behaviour is either missing or limited. Pressure pedestal analysis at JET [3, 4, 8] indicated indirectly that poloidal Larmor radius of the fast particles lost to the edge could determine the width of the pedestal pressure, p_{ped}. It was later shown, with the same indirect pedestal pressure analysis [2] but in a more extensive study, where long pulse high q_{95} discharges with IC and NBI heating were compared at the same density, that the pedestal width did not depend on the fast particles Larmor radius. Ref. [2] finds similar ELM frequency, f_{ELM}, and $p_{ped,}$ for IC and NB H-modes, while [3] reports higher f_{ELM} and lower p_{ped} with IC.

The limited number of IC dominated Type I ELMy H-modes in the JET databases is due to the difficulties in coupling IC power with these ELMs. The experiment described in this paper is aimed at comparing Type I ELMy H-modes with dominant IC and dominant NB heating in a relevant JET H-mode operational space, i.e. in a range of plasma parameters that are comparable to the bulk of JET data for confinement, pedestal and ELM studies. This experiment was made possible by the availability of the ITER relevant ELM resilient systems (3dB and conjugate-T) installed in the JET A2 antenna and of the new JET ITER like (ILA) antenna [9]. The new JET High resolution Thomson scattering provided pedestal data that was not available in previous experiments.

2. The experiment

The scope of this experiment in JET was to compare pedestal/ELMs and core confinement and transport of Type I ELMy H-modes with IC and NB heating, in a relevant H-mode operational space in terms of plasma current, I_p (=2.5MA), q_{95} (=3.6) and density (=60-70% of the Greenwald density n_G). In order to maximise the coupled IC power, H minority heating at B_t=2.7T with 42 MHz dipole phasing was used, allowing a all the JET ELM-resilient systems, including the new ILA antenna [9], to be employed together. In addition, a standard low triangularity (i.e ($<\delta>$=0.25) plasma configuration was chosen, as having good coupling characteristics. These choices allowed up to 9MW of IC power to be reliably coupled in a typical JET Type I ELMy H-mode.

H-modes heated only by NB where compared with H-modes with 50:50 IC: NB, with loss power of ~ 16 MW, about twice the L-H threshold power. Comparisons were also done at lower levels of total power, down to ~1.2 the L-H threshold power and with various IC proportions, up to 100% IC. The bulk of the comparisons were done with a density of ~ 65% of the Greenwald-density (n_G), corresponding to ~5.7 10^{19} m^{-3}. This density is slightly higher than the natural density for NB H-modes with this plasma configuration, which is ~60% n_G, because some base level of external gas fuelling with D_2 and/or H_2, the latter for minority heating, was maintained in both NB and IC H-modes. The Hydrogen concentration, as measured at the edge, was maintained to 4±0.5% for all H-modes, even for those with NB only. Furthermore, experiments were done at a higher density of (~70% of n_G) via increased D_2 gas fuelling. Since the NB system also provides fuelling, some IC comparisons at constant power were carried out with the same fuelling rate used with NB. Furthermore, discharges with combined IC and NB heating with powers up to 24MW were achieved.

3. General results

The overall comparison of the confinement of H-modes with NB and with combined heating at different fractions (≥50%) of IC power, different levels of total power and different density shows that the thermal energy confinement enhancement factor $H_{98}(y)$ does not depend on the heating mix, as seen in Fig. 1. As usually found at JET the H-factor decreases with increasing density. Some further degradation of the energy confinement is seen when the total additional heating power is reduced. This aspect is discussed in section 5.

A more detailed comparison between H-modes heated by NB and by predominant IC was carried out by studying matching pairs of H-modes at similar density and power, but with a different heating mix. The

divertor D_α traces of these pairs of H-modes with decreasing levels of total power are shown in Fig. 2a for IC + NB, and in Fig. 2b for NB heating only. In the H-modes with combined IC and NB heating, the IC power was kept constant while decreasing the total power, therefore the IC proportion increases as the power decreases The IC proportion is 50% at 16MW total power and increases up to 100% IC at ~9MW(Fig. 2a). IC fraction and loss power are therefore not independently varied in the experiment.
No obvious correlation between ELM frequency (f_{ELM}) and additional heating mix is found. In fact, f_{ELM} is lower in the NB heating case compared to combined heating at 16 MW, but it is higher with NB at 13 MW. Z_{eff} varies from 1.7 to 2 in all the pairs of H-modes of the comparison, apart from the NB only case with the highest loss power, where it has the slightly higher value of ~2.5.

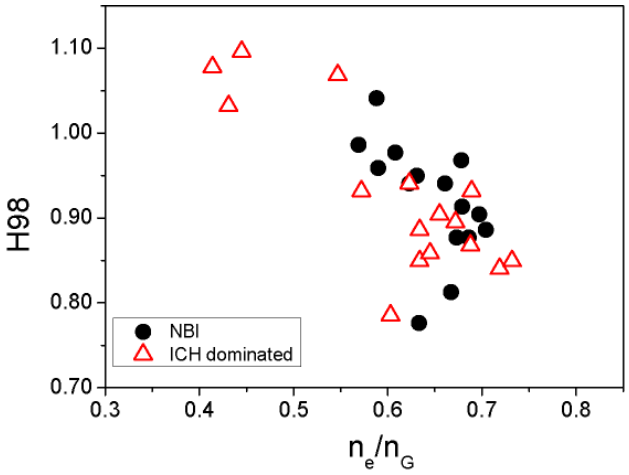

***Figure 1**: Energy confinement enhancement factor versus normalised density n_e/n_G. In black are the points for H-modes heated only by NBI and in red are H-modes where 50% or more of the additional heating is provided by IC.*

In order to maintain the same density, a 3 times higher gas rate (~$1.5\cdot10^{22}$ compared to ~$0.5\cdot10^{22}$ electrons/s) was necessary with IC+NB than with NB heating only in the matched pair of discharges at 16 MW. The H-mode with 50% IC was repeated with the same lower gas fuelling as in the comparable NB plasma, and in this case the density decreased from 60% to 45%n_G. For all the other comparison pairs at lower power (lower NB) instead, similar density was obtained with the same gas flow of 1.5 10^{22} electrons/s.

Common to all the pairs that reach the same density is the fact that an approximate fuelling balance, carried out assuming a fuelling efficiency of 0.9 for NB fuelling and of 0.1 for gas fuelling, shows that the difference between the total external fuelling flux in the IC and NB plasmas is ~10^{20} s^{-1}, much lower than the recycling flux of ~10^{22} s^{-1}. ELM loss analysis shows that the ELM power fluxes (calculated as $<\Delta W_{ELM}> f_{ELM}$, MW) are comparable in the IC and NB pairs, despite the different ELM frequency. Therefore it is not unreasonable to assume that also the ELM particle flux is similar. Therefore when lower density is obtained with IC, this seems to be due predominately to the lower external fuelling and not to changes in ELM particle losses.

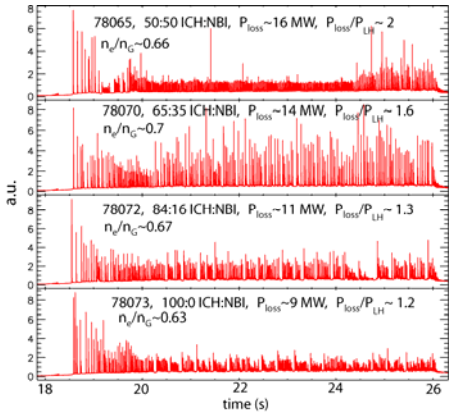

***Figure 2a:** Combined heating H-modes (IC and NBI) with varying proportion of IC power (from 50 to 100% IC), and varying total input power (from ~16 MW to ~9 MW). At each level of power, apart from the 9 MW, the corresponding comparison H-mode with NBI only is shown in Fig. 2b.*

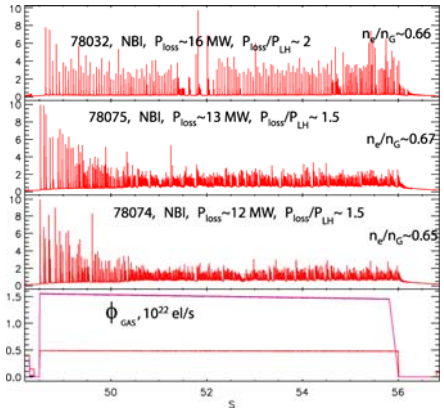

***Figure 2b**: H-modes heated only by NBI with varying total input power (from ~16 MW to ~12 MW). At each level of power the corresponding comparison H-mode with NB+IC only is shown in Fig. 2a. The Figure also shows that the two levels fuelling flux ϕ_{gas}, the lower one for the H-mode at 16 MW, the highest one for the others as well as for the comparison H-modes in Fig. 2a.*

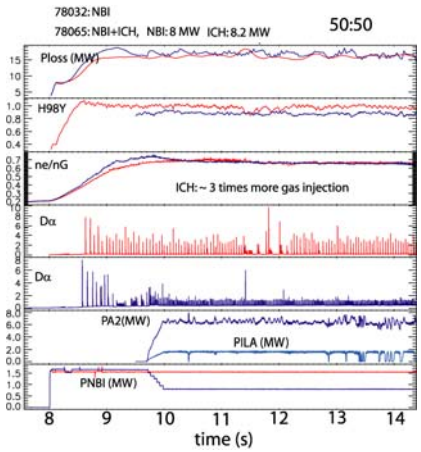

***Figure 3a**: Time traces of the main plasma parameters for the H-modes at 16 MW with NB only and with ~50:50 IC:NB.*

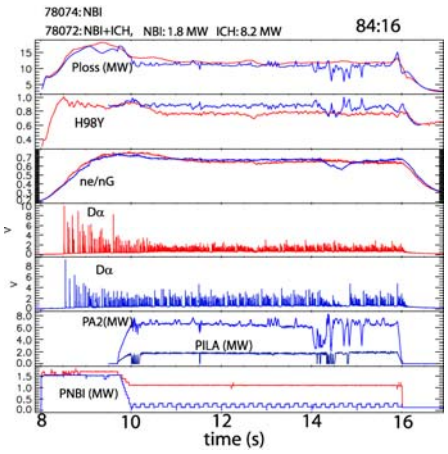

***Figure 3b**: Time traces of the main plasma parameters for the H-modes at 11MW with NB only and with ~85:15 IC:NB.*

Fig. 3a and 3b show the main plasma parameters for the comparison pairs with 50:50 IC:NB (16 MW) and with ~84:16 IC:NB. As indicated by Fig. 1, the differences in energy confinement enhancement factors within the pairs are at most 10% at similar density and not systematic. In fact at 16 MW the NB H-mode has higher H_{98}, while at 11 MW the IC H-mode has higher confinement enhancement factor.

4. Transport and confinement

Core density and temperature profiles with predominant IC or NB heating are similar for all the comparison pairs at similar density and power of Fig. 2a and 2b. This is shown in Fig. 4 for the H-mode with 85% IC (Fig. 4a and 4b) and for the H-mode with 50% IC (Fig. 4c). Some increase in the ion (T_i) and electron temperatures (T_e) profiles inside the sawtooth inversion radius, which corresponds to <20% of the plasma volume, is observed with predominant IC. In all these H-modes at relatively high density, ion and electron temperatures are similar. The largest difference between T_e and T_i is less that 20% with the highest NB power of 16 MW.

Similar confinement and core profiles are obtained with different power deposition profiles: mainly off axis with NB, and mainly on axis with predominant IC as shown in Fig. 5a for the H-mode with 85% IC. In fact, by changing the total power, the beam energy and, more importantly, the beam to IC proportion, the power deposition profiles were changed significantly during the experiment. With pure NB heating, the fraction of power deposited inside ρ=0.5 is typically of the order of 40% of the total, increasing to 60% of the total with 50% IC. Fig. 5a shows for the comparison between pure NB and 84% IC heating. The latter produces an extremely peaked power deposition, with up ~85% of the power deposited inside mid-radius.

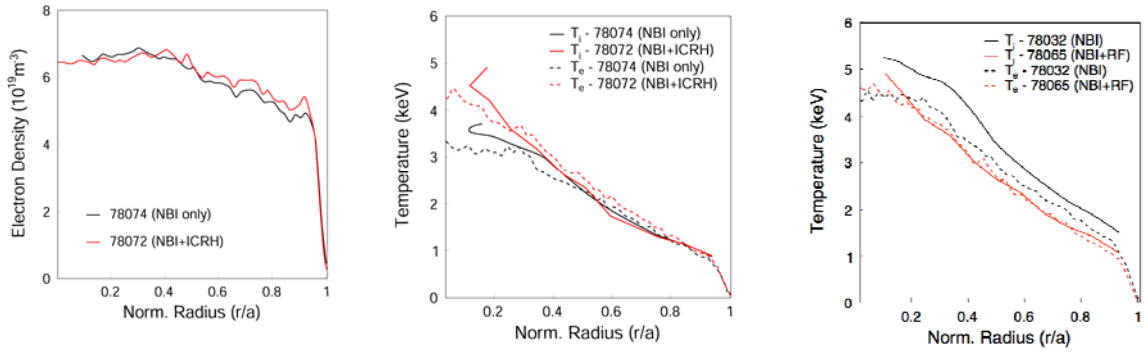

***Figure 4**: a) (left) Electron density profiles from the HRTS diagnostic for the H-modes with NB only (black) and with 85% IC (red) shown in Fig. 2a. b) (middle) Ion (from Charge Exchange recombination spectroscopy) and electron (from HRTS) temperature profile the H-modes with NB only (black) and with 85% IC (red) shown in Fig. 2a. c) (right) Ion (from Charge Exchange recombination spectroscopy) and electron (from HRTS) temperature profile for H-modes with NB only (black) and with 50% IC (red).*

To put this in perspective, the power deposition in the baseline Q=10 ITER scenario (including α particles) is predicted to have ~70% on the power deposited on ions and electrons within mid radius. The power to ions and electrons also changed significantly with increased IC fraction; with ~14% more power to the ions with only 50% IC heating while when the IC fraction was increased to 85%, the electrons received 40% more power. While for the NB case, as shown in Fig. 5b, the power was equally distributed over the ions and electrons.

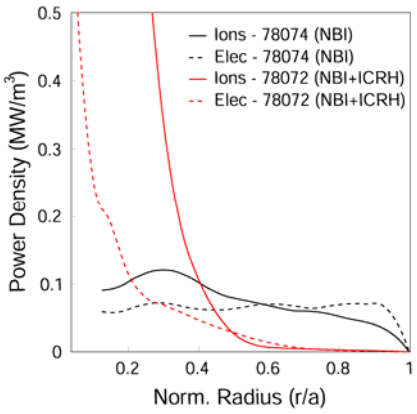

***Figure 5a**: Power density to ions and electrons for the same H-modes of Fig. 4a, with NB only (black) and with 85% IC (red)*

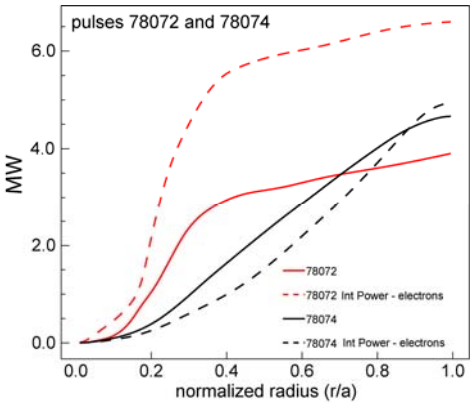

***Figure 5b**: Integrated power to ions and electrons for the same discharges as Fig. 5a, with NB only (black) and with 85% IC (red)*

The reduction of the NB fraction, and hence the torque, also resulted in a significant drop in plasma toroidal rotation, ω_{tor}. High IC fraction discharges had a ~5 times lower ω_{tor} in the core and ~10 times lower values in the edge compared to NB heating, as shown in Fig. 6a. The Mach number dropped from ~0.4 with NB heating to <0.1 at 100% IC. Interpretative transport analysis was carried out with the JETTO code for two comparison pairs, with a power of 16 MW and 50:50 IC:NB and a power of 11 MW with 85:15, respectively. The effective ion and electron heat diffusivities for the same H-modes are shown in Fig. 6b. The larger core power deposition, when the IC fraction was increased, did not lead to a difference in ion temperature profiles, suggesting that these profiles are generally stiff. The increased heat flux leads to larger effective heat diffusivity in the gradient region as shown in Fig. 6b.

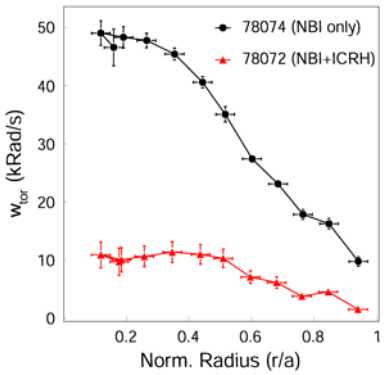

***Figure 6a**: Toroidal rotation profile from Charge Exchange recombination spectroscopy for the same H-modes of Fig. 4a with NB only (black) and with 85% IC (red)*

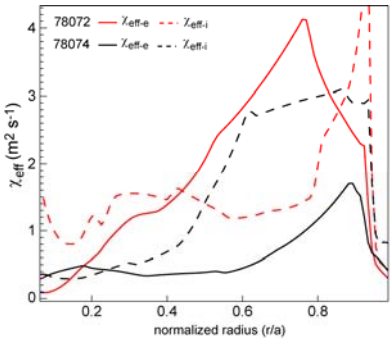

***Figure 6b**: ion and electron effective heat diffusivities for the same H-modes as Fig. 6a with NB only (black) and with 85% IC (red)*

A more detailed evaluation of the profile stiffness for all the discharges reveals, however, that stiffness varied in this experiment. In Fig 7 the normalised ion heat flux is plotted against the normalised inverse ion temperature gradient length, similarly as done in Ref. [7]. The data are separated by the value of the toroidal rotation gradient, fraction of IC power, and level of total power.

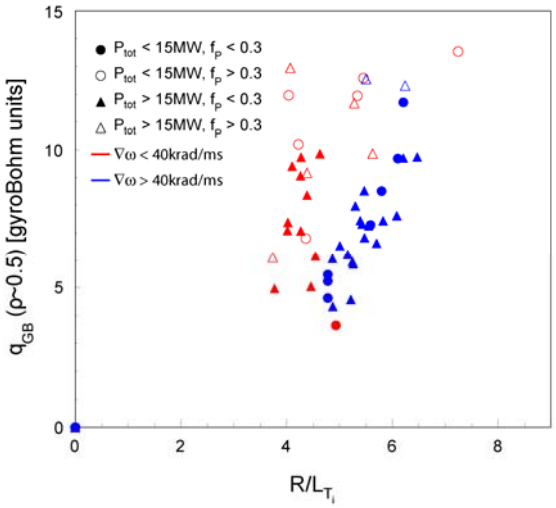

***Figure 7**: Normalised heat flux in Gyro-Bohm units versus normalised inverse gradient length of the ion temperature. The points are coloured to highlight two different levels of grad ω, the different symbols differentiate the levels of power and the different levels of IC fraction, fp=P_{IC}/(P_{IC}+P_{NB}), are highlighted with full and empty symbols*

As expected, the high rotation data is mostly populated by low IC fraction, while the high normalised heat flux region of the plot is mostly populated by high IC fraction. The trend indicates that those discharges with a higher rotation have a larger normalised ion temperature gradient length The interpretation of these data is not unambiguous, in particular due to the large error in the gradient data (~40%), as well as to the spread of the low rotation data. For example, such a trend is not clearly visible in the ion temperature profiles shown in Fig. 2c, which shows similar profiles for different IC fractions and rotation levels. Furthermore the small differences in inverse gradient length did not lead to significant differences in the overall temperature profiles and in the global confinement properties of the plasma. In addition, this analysis does not include the pedestal, which plays an important role in the global confinement of an ELMy H-mode.

5. Pedestal and ELMs

The pedestal analysis was carried out using density and temperature profile data obtained by High Resolution Thompson Scattering (HRTS) and by ECE diagnostics for the temperature data, and further information on the density from the FIR interferometer. The comparison of the pairs of H-modes with NB and with combined heating shows that the pedestal pressure does not depend on the heating mix. This is illustrated in Fig. 8, which shows the n_e-T_e diagram for the pairs of matched H-modes of Fig. 2, with the addition of few points representing H-modes at lower and higher density than the comparison pairs, to illustrate the density dependence.

An average constant pressure line is drawn in Fig. 8. The points follow this constant pressure line as the density is increased. The figure shows also that, independent of additional heating mix, a group of data deviates from the constant pressure, towards lower temperature. These discharges show a decrease of H_{98} when the density is increased at constant power (figure 9). This is due to two factors that are seen either separately or combined. Firstly, the scaling predicts an increase of stored energy with density, while instead both pedestal and total stored energy remain constant in the experiments, therefore H_{98} decreases. Secondly, a decrease of pedestal temperature with density stronger than T∝1/n, which is seen in JET mostly at low triangularity, produces a lower total stored energy.

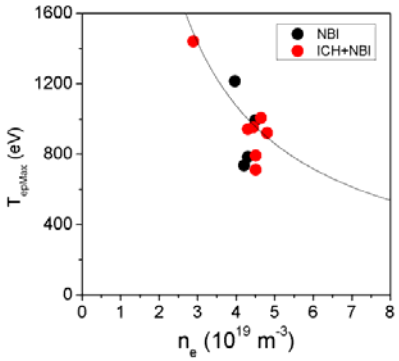

***Figure 8**: ne-Te diagram for IC dominated (in red) and NB heated H-modes.*

It is therefore not surprising that H_{98} is seen to decrease with density here, even with approximately constant pressure. The deviation of the pedestal data from constant pressure in Fig. 8, which is correlated with the decrease in H_{98} at almost constant density, is observed when the loss power is decreased from ~16 to ~9MW, both with NBI and with IC, as illustrated in Fig. 10. The degradation of p_{ped} with decreasing power, independent of heating mix, is due to a decrease of pedestal temperature as illustrated in Fig. 11 for both HRTS and ECE data. The decrease of

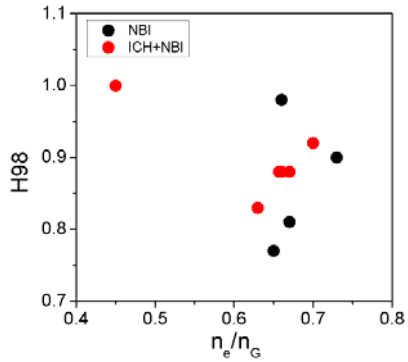

***Figure 9**: the H factor as a function of normalised density n_e/n_G for the same H-modes as figure 8*

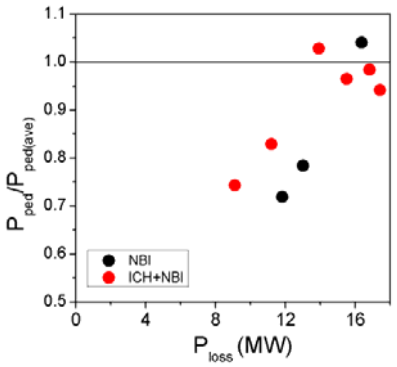

***Figure 10**: Pedestal pressure normalised to the constant pressure value of Fig. 8, showing that the decrease in pedestal pressure is due to the decrease in input power*

pedestal temperature with power is also independent of heating mix. This effect could be specific of the low triangularity configuration used in this experiment, and related to the fact that, by decreasing the power, the margin above the threshold power was also decreased. Not only the pedestal pressure and its trends are similar with different heating mix, the pedestal temperature (and density) widths are found to be independent of heating mix, as shown in Fig. 12. Therefore the temperature and density pedestal widths are also independent of power.

Although the ELM frequency varies between H-modes with NBI and with predominant IC at the same power, this variation is not correlated with changes in heating mix. Even if the ELM frequency f_{ELM} can be different, the comparison of the pairs of H-modes at the same total power and density, with NBI and with dominant IC, shows that the power loss by the ELMs, $f_{ELM}\Delta W$ is the same for a given power. The power loss by the ELM is also seen to increases with power. In summary, the pedestal is similar with IC and NB and has similar trends and the variation of H-factor reflects changes in the pedestal in both cases, as normally seen in ELMy H-modes

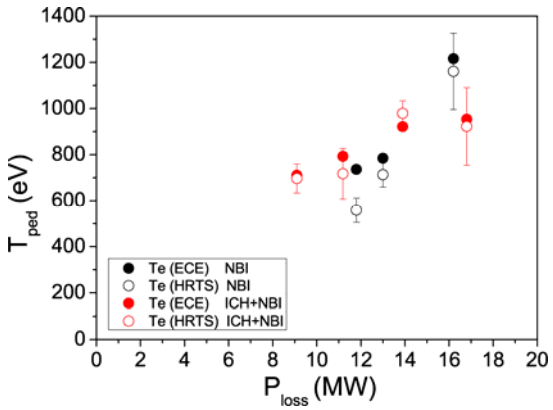

***Figure 11**: Pedestal temperature versus loss power for all the pairs of comparable H-modes with NB (black) or predominant IC (red). The point at lower temperature is the 100% IC which has no NB comparisons at the same power*

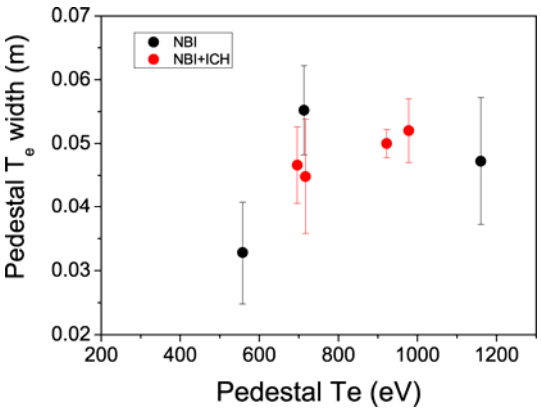

***Figure 12**: Width of the pedestal temperature for the same discharges in Fig. 10*

6. Discussion and conclusion

The experiment described in this paper aimed to characterize ELMy H-mode for plasmas with varying momentum input, rotation, power deposition profiles and ion to electron heating ratio obtained by varying the additional heating mix. The motivation was the verification that the basic plasma confinement properties of the baseline ITER Q=10 H-mode scenario are similar to those derived from the large database of NB heated H-modes, where heating is normally associated to large momentum input, coupling between injected power and rotation, as well as with core fuelling.

The power deposition profiles varied from very peaked (~85% power inside ρ=0.5) with predominant IC, to flat deposition for pure NBI cases. The plasma toroidal rotation was varied by a factor of ~5 in the core and ~10 in the edge. Those variations did not produce any significant difference in the density and temperature profiles or in the global confinement. An analysis of the variations of the normalised ion temperature gradient length with normalised ion heat flux showed that in general ion temperature were stiff. Albeit a small variation in stiffness was found, dependent on the plasma rotation, similar as reported in [7]. These variations had, however, no significant effect on the global confinement. The impact of rotation of the ion temperature profile stiffness is also thought to be limited in the presence of large magnetic shear, such as in these discharges with fully developed q-profiles [10].

This analysis shows the thermal plasma energy confinement enhancement factor to be independent of the heating mix, for the range of conditions explored. Moreover, the response of the global confinement to changes in density and power, and the consequent variations of H_{98}, were also seen to be independent of heating mix. The H_{98} factor was seen to decrease with density, as normally seen in ELMy H-modes, and with power, at low power above the threshold power. These variations are mainly reflecting changes in the pedestal. The pedestal characteristics (pressure and width) and their dependences were found to be independent of heating mix. Observed variations in global confinement were mainly reflected by changes in pedestal pressure (or temperature).

Finally, the range of power deposition profile, ion to electron power deposition, core fuelling and momentum injection are inclusive of what we expect for ITER in the baseline H-mode scenario. The results presented here indicate that the global confinement scaling at the basis of the ITER Q=10 performance prediction is robust in spite of having being derived from a majority of plasma H-modes with high momentum input, prevalent ion heating and relatively flat deposition profiles.

Acknowledgements
This work was supported by EURATOM and carried out within the framework of the European Fusion Development Agreement. The views and opinions expressed herein do not necessarily reflect those of the European Commission.

The views expressed in this publication are the sole responsibility of the author and do not necessarily reflect the views of Fusion for Energy. Neither Fusion for Energy nor any person acting on behalf of Fusion for Energy is responsible for the use which might be made of the information in this publication.

References
[1] DE VRIES, P.C., et al. Nuclear Fusion. **48** (2008) 065006
[2] JET TEAM (prepared by FG Rimini and G Saibene), Nuclear Fusion **42** (2002) 86
[3] LINGERTAT, J., et al., Journal of Nuclear materials **124-130** (1999) 266
[4] BHATNAGAR, V.P., et al., Nuclear Fusion **39** (1999) 353
[5] SUTTROP, W., et al., in the Proc. of the EPS Conf. on Plasma Physics (Madeira, Portugal, 2001)
[6] STÄBLER, A., et al., Nuclear Fusion **45** (2005) 617
[7] MANTICA, P., et al., Phys. Rev. Letters **102** (2009) 175002
[8] PARAIL, V.V, GUO, H.Y., J. LINGERTAT, J, Nuclear Fusion **39** (1999) 369
[9] DURODIE, F., et al., this conference EXW/P7-0
[10] MANTICA, P., et al., this conference EXC/9-2